Supporting information:

Emission behavior, Enol-Keto tautomerism and bioactivity of hydroxy-substituted cyclic chalcone derivatives

Jiaxin Zhao, Jian Zhao*, Xinrui He, Zeqing Tan, Xiao Cheng*, Qiuju Han*, Chuanjian Zhou*

Experimental Section

Materials and Instruments.

o-Phthalaldehyde (98%) was obtained from Aladdin, 1-(4-(dimethylamino)phenyl)ethanone (97%) was obtained from Macklin, 1-(4-(diphenylamino)phenyl)ethanone (97%) was obtained from Amatek, 1-(4-(9H-carbazol-9-yl)phenyl)ethanone (98%) was obtained from ATK Chemical, all the other ingredients were obtained from Sinopharm Chemical Reagent, and were used without further purification.

Synthesis procedure

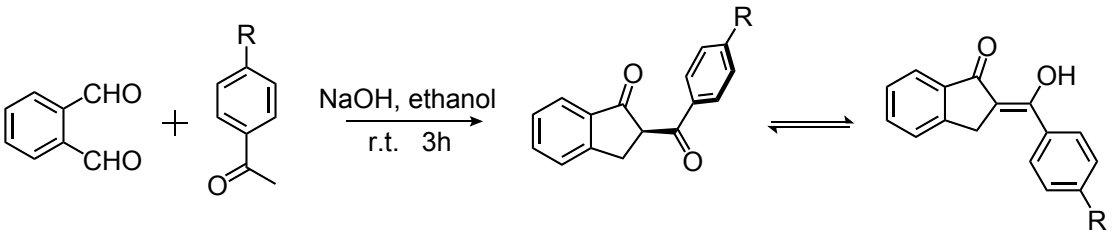

Scheme S1. Synthesis procedure and enol-keto tautomerization of compounds 1-3.

Compounds 1-3 are synthesized according to literature.1 The procedure is shown in Scheme S1. In a round bottom flask, the raw materials 1:1 were mixed and fully dispersed in ethanol solution and 1.5 times equivalent sodium hydroxide was added as a catalyst. Then the mixture was stirred at room temperature for 3 hours. After the reaction, dilute hydrochloric acid is used to neutralize and precipitate the product. The precipitates were filtered out, washed with water and cold ethanol, and then dried as a crude product. The yield of crude product is about 50%-70%. Three corresponding crystals were obtained by volatilizing concentrated dichloromethane solution in a test tube. The structure and composition of the crystal were characterized by NMR, MS, elemental analysis and SCXRD.

NMR spectra were recorded on a Bruker Avance 500 MHz spectrometer with tetramethylsilane as the internal standard, while mass spectra were recorded on a Bruker ultra-performance LC coupled to Q-TOF mass spectrometer. Elemental analyses were performed on an Elementar Vario EL Cube spectrometer. UV-vis absorption spectra were recorded on a Shimadzu UV-2600 spectrophotometer. Emission spectra were recorded using a Shimadzu RF-6000 spectro fluorophotometer. Absolute fluorescence quantum yields and fluorescent lifetime were recorded with Horiba Scientific DeltaHub and Quanta-ϕ. Microscopy images were measured on Axio Observer 3 inverted fluorescence microscope. All measurements were carried out at room temperature under ambient conditions.

2-(P-dimethylamino) benzoyl-1-indenone (**1**). Yield: 54%. ^{1}H NMR (300 MHz, $CDCl_3$, δ): Enol tautomer (66%) 15.59 (s, 1H), 8.03 (d, *J* = 9.0 Hz, 1H), 7.95(d, *J* = 9.0 Hz, 2H), 7.86 (d, *J* = 9.0 Hz, 1H), 7.53 (m, 2H), 6.85 (d, *J* = 9.0 Hz, 2H), 3.94 (s, 2H), 3.09 (s, 6H); diKetone tautomer (34%) 7.71 (d, *J* = 9.0 Hz, 1H), 7.61 (m, 1H), 7.55 (m, 1H), 7.42 (m, 1H), 7.36 (t, *J* = 6.0 Hz, 1H), 6.73 (d, *J* = 9.0 Hz, 2H), 4.78 (q, 1H), 3.94 (m, 2H), 3.09 (m, 6H); ^{13}C NMR (125 MHz, $CDCl_3$, δ): 201.17, 193.91,

191.78, 172.34, 154.74, 153.67, 152.17, 147.90, 138.41, 135.67, 134.98, 132.40, 132.13, 130.12, 127.45, 127.21, 126.51, 125.35, 124.45, 122.90, 111.42, 110.73, 107.52, 55.85, 40.07, 32.97, 30.23. MS m/z: [M]+ calcd for $C_{18}H_{17}NO_2$: 279.34; found: 280.12. Anal. calcd (%) for $C_{18}H_{17}NO_2$: C, 77.40; H, 6.13; N, 5.01; found: C, 77.14; H, 6.11; N, 4.98.

2-(P-diphenylamino) benzoyl-1-indenone (**2**). Yield: 62%. ^{1}H NMR (500 MHz, $CDCl_3$, δ): Enol tautomer (72%) 15.38(s, 1H), 7.85 (d, *J* = 10 Hz, 2H), 7.33 (m, 5H), 7.17 (m, 9H), 7.08 (d, *J* = 10 Hz, 2H), 3.93 (s, 2H); diKetone tautomer (28%) 7.96 (d, *J* = 10.0 Hz, 2H), 7.87 (d, *J* = 10 Hz, 2H), 7.72 (d, *J* = 10 Hz, 1H), 7.62 (t, *J* = 5.0 Hz, 1H), 7.55 (m, 6H), 7.43 (m, 3H), 7.37 (m, 2H), 7.02 (d, *J* = 5.0 Hz, 1H), 4.77 (q, 1H), 3.93 (s, 2H); ^{13}C NMR (125 MHz, $CDCl_3$, δ): 194.94, 170.97, 154.62, 152.55, 150.80, 148.15, 146.59, 146.32, 138.19, 135.16, 132.88, 131.55, 129.67, 129.62, 129.54, 127.59, 127.37, 126.72, 126.53, 126.25, 125.84, 125.47, 124.89, 124.56, 124.51, 123.19, 120.38, 119.21, 108.35, 56.19, 32.7. MS m/z: [M]+ calcd for $C_{28}H_{21}NO_2$: 403.48; found: 404.15. Anal. calcd (%) for $C_{28}H_{21}NO_2$: C, 83.35; H, 5.25; N, 3.47; found: C, 83.81; H, 5.27; N, 3.45.

2-(P-carbazolyl) benzoyl-1-indenone (**3**). Yield: 67%. ^{1}H NMR (500MHz, $CDCl_3$, δ): Enol tautomer (83%) 15.18 (s, 1H), 8.22 (d, *J* = 10.0 Hz, 2H), 8.16 (d, *J* = 5.0 Hz, 2H), 7.94 (d, *J* = 10.0 Hz, 1H), 7.76 (d, *J* = 10.0 Hz, 2H), 7.53 (m, 7H), 7.33 (m, 2H), 4.06 (s, 2H); diKetone tautomer (17%) 8.41 (d, *J* = 10.0 Hz, 2H), 8.16 (m, 1H), 7.77 (m, 2H), 7.67 (t, *J* = 5.0 Hz, 2H), 7.53 (m, 7H), 7.33 (m, 2H), 4.95 (q, 1H), 3.94 (m, 2H); ^{13}C NMR (125 MHz, $CDCl_3$, δ): 199.92, 196.02, 192.93, 169.50, 148.52, 140.45, 140.33, 137.87, 135.48, 133.55, 133.36, 131.79, 129.82, 127.82, 127.62, 126.66, 126.32, 126.26, 126.20, 125.67, 124.75, 123.79, 123.58, 120.69, 120.55, 120.48, 109.93, 109.81, 109.64, 56.77, 32.37. MS m/z: [M]+ calcd for $C_{28}H_{19}NO_2$: 401.47; found: 402.16. Anal. calcd (%) for $C_{18}H_{17}NO_2$: C, 83.77; H, 4.77; N, 3.49; found: C, 83.27; H, 4.75; N, 3.46.

Single-crystal X-ray Diffraction.

Single-crystal X-ray diffraction data were collected on a Rigaku RAXIS-PRID diffractometer in ω-scan mode using graphite-monochromated Mo-Kα radiation. Structures were solved with direct methods using the SHELXTL program and refined with full-matrix least squares on F^2. Non-hydrogen atoms were refined anisotropically, while the positions of hydrogen atoms were calculated and refined isotropically. [CCDC 2013934-2013936 for **1**–**3** contain the supplementary crystallographic data for this paper. These data can be obtained free of charge from The Cambridge Crystallographic Data Centre via www.ccdc.cam.ac.uk/data_request/cif.]

Computational details.

All geometries are optimized at Becke's three-parameter hybrid exchange function with the Lee–Yang–Parr gradient-corrected correlation functional (B3LYP) method and def2-TZVPP[2] basis set with Grimme's DFT-D3(BJ) empirical dispersion correction[3] by Gaussian 09 software[4]. And the frequency calculations of favored and transition-state structures were performed at the same level to guarantee that there is no and only one imaginary frequency, which corresponds to the true minima and saddle point on the potential energy surfaces. The implicit solvents were employed for all geometries with SMD (Solvation model density) solvation model[5]. And molecular transition states were performed with rational function optimization (RFO)[6, 7], and intrinsic reaction coordinate (IRC)[8, 9] was used to verify that we have the correct transition state at B3LYP/def2-TZVPP level of theory. Furthermore, the single point energy of all molecules were performed at B3LYP-D3(BJ)/def2-QZVPP level of theory. The absorb energy was calculated at TD-B3LYP-D3(BJ)/def2-TZVPP[10-16] at the structure of ground state, while re-optimized at the same level for those of emission ones. The HOMO and LUMO were viewed by VMD 1.9.3[17], whose

input files were extracted from Multiwfn 3.7[18].

Cell imaging details.

Cell culture. Human cell lines including HEK (human embryonic kidney) 293 and lung cancer A549 cells were purchased from the Cell Bank of Type Culture Collection of the Chinese Academy of Sciences and conserved in our lab. Cells were cultured in RPMI 1640 with 10% (v/v) fetal bovine serum, and incubated in a humidified incubator with 5% CO_2 at 37°C.

Cell Imaging. Both HEK293 and A549 cells were incubated with different concentrations (20 μM, 50 μM, 100 μM) of Compound 1 for 24h. Then, the cells were imagined by fluorescence microscope, and the excitation wavelength was 488 nm.

MTT assay. Briefly, A549 cells (8×10^3) were plated in a 96-well plate, allowed to adhere for 4 hours, then treated with different concentrations of Compound 1 at the indicated time points (24 and 48 h). 0.5% MTT solution was added to each well and incubated for 4 hours. DMSO was then added to extract the formazan, and the optical density was read at 490 nm.

Cell cycle and Apoptosis analysis. A549 cells were seeded in 12-well plates at a density of 2×10^5 per well. The following day, cells were treated with Compound 1 (100 μM), control wells were treated with equal volumes of DMSO. After 48 hours of treatment, cells were harvested and washed twice, then fixed with 70% ethanol at 4°C overnight. The cells were washed with PBS twice and incubated with DNase-free RNase A (Solarbio, China) at a concentration of 100 mg/ml for 30 min, then stained with propidium iodide (PI, 50 μg/mL, Solarbio, China) for 30 min at room temperature in the dark, at last cell cycle analysis was performed using a flow cytometer. To determine rates of apoptosis, cells underwent the same treatment were stained with Annexin V-fluorescein isothiocyanate (FITC)/PI according to the manufacturer's protocol.

Reference

1 M.L. González, M.E. Sánchez-Vergara, J.R. Álvarez-Bada, M.I. Chávez-Uribe, R.A. Toscano and C. Álvarez-Toledano, J. Mater. Chem. C, 2014, 2, 5607-5614.
2 S. Grimme, S. Ehrlich and L. Goerigk, J. Comput. Chem., 2011, 32, 1456-1465.
3 L. Goerigk and S. Grimme, J. Chem. Theory Comput., 2010, 7, 291-309.
4 M.J. Frisch, G.W. Trucks, H.B. Schlegel, G.E. Scuseria, M.A. Robb, J.R. Cheeseman, G. Scalmani, V. Barone, B. Mennucci, G.A. Petersson, H. Nakatsuji, M. Caricato, X. Li, H.P. Hratchian, A.F. Izmaylov, J. Bloino, G. Zheng, J.L. Sonnenberg, M. Hada, M. Ehara, K. Toyota, R. Fukuda, J. Hasegawa, M. Ishida, T. Nakajima, Y. Honda, O. Kitao, H. Nakai, T. Vreven, J.A. Montgomery Jr, J.E. Peralta, F. Ogliaro, M.J. Bearpark, J. Heyd, E.N. Brothers, K.N. Kudin, V.N. Staroverov, R. Kobayashi, J. Normand, K. Raghavachari, A.P. Rendell, J.C. Burant, S.S. Iyengar, J. Tomasi, M. Cossi, N. Rega, N.J. Millam, M. Klene, J.E. Knox, J.B. Cross, V. Bakken, C. Adamo, J. Jaramillo, R. Gomperts, R.E. Stratmann, O. Yazyev, A.J. Austin, R. Cammi, C. Pomelli, J.W. Ochterski, R.L. Martin, K. Morokuma, V.G. Zakrzewski, G.A. Voth, P. Salvador, J.J. Dannenberg, S. Dapprich, A.D. Daniels, Ö. Farkas, J.B. Foresman, J.V. Ortiz, J. Cioslowski and D.J. Fox, 2009.
5 A.V. Marenich, C.J. Cramer and D.G. Truhlar, The Journal of Physical Chemistry B, 2009, 113, 6378-6396.
6 BANERJEE, N. ADAMS, J. SIMONS and R. SHEPARD, JOURNAL OF PHYSICAL CHEMISTRY, 1985, 89, 52-57.
7 J. Simons and J. Nichols, Int. J. Quantum Chem., 1990, 38, 263-276.
8 K. Fukui, Accounts Chem. Res., 1981, 14, 363-368.
9 H.P. Hratchian and H.B. Schlegel, In: Theory and Applications of Computational Chemistry: The First 40 Years. Edited by C. E. Dykstra, G. Frenking, K. S. Kim, and G. Scuseria, Amsterdam: Elsevier, 2005.
10 G. Scalmani, M.J. Frisch, B. Mennucci, J. Tomasi, R. Cammi and V. Barone, The Journal of Chemical Physics, 2006, 124, 94107.
11 R. Bauernschmitt and R. Ahlrichs, Chem. Phys. Lett., 1996, 256, 454-464.
12 M.E. Casida, C. Jamorski, K.C. Casida and D.R. Salahub, The Journal of Chemical Physics, 1998, 108, 4439-4449.

13 R.E. Stratmann, G.E. Scuseria and M.J. Frisch, The Journal of Chemical Physics, 1998, 109, 8218-8224.
14 Van Caillie and R.D. Amos, Chem. Phys. Lett., 1999, 308, 249-255.
15 Van Caillie and R.D. Amos, Chem. Phys. Lett., 2000, 317, 159-164.
16 F. Furche and R. Ahlrichs, The Journal of Chemical Physics, 2002, 117, 7433-7447.
17 W. Humphrey, A. Dalke and K. Schulten, Journal of Molecular Graphics, 1996, 14, 33-38.
18 T. Lu and F. Chen, J. Comput. Chem., 2012, 33, 580-592.

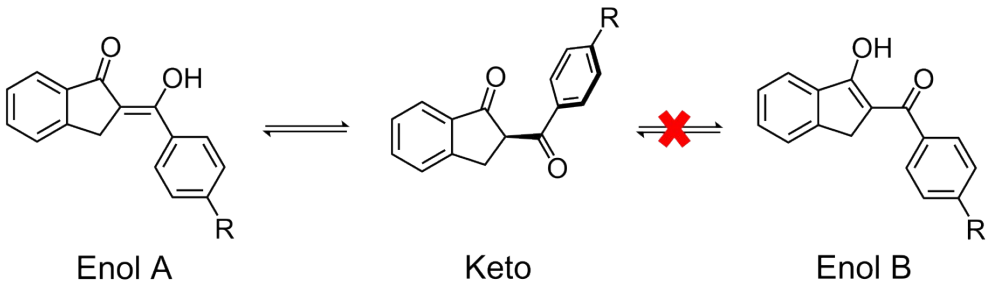

Figure S1. Three theoretically-existed molecular configurations: Enol A, Keto, Enol B. Enol A and Keto form have been proved experimentally while Enol B is nonexistent.

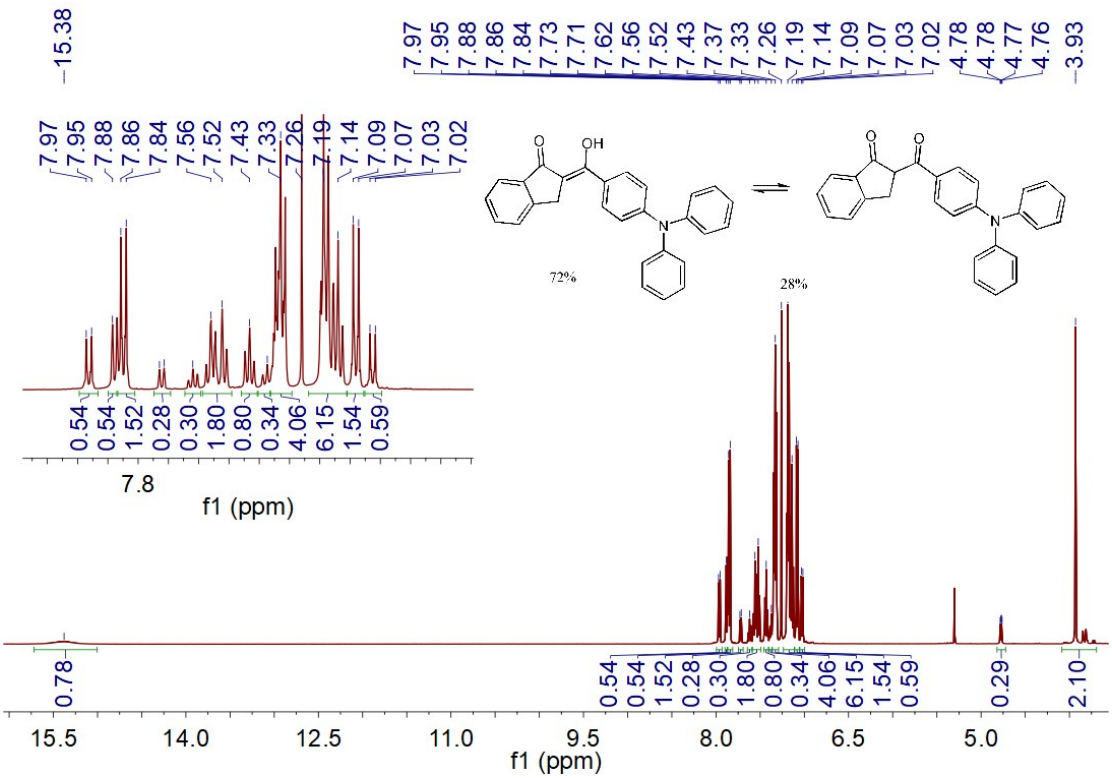

Figure S2. ^{1}H NMR spectrum for compound **2** in $CDCl_3$ (500 MHz, 298K).

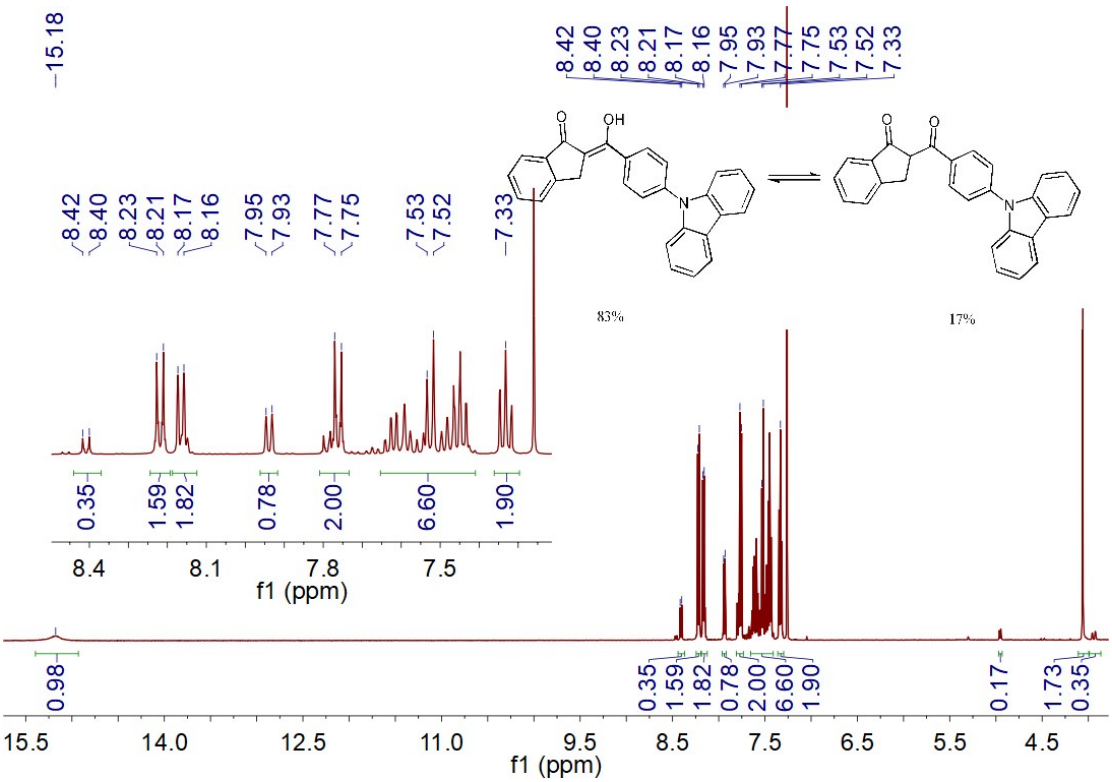

Figure S3. ^{1}H NMR spectrum for compound **3** in $CDCl_3$ (500 MHz, 298K).

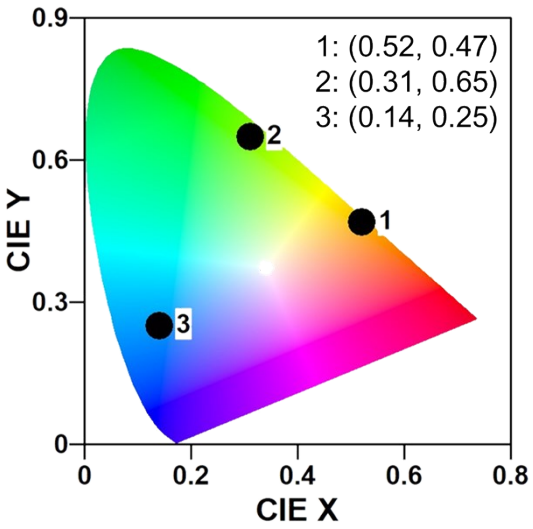

Figure S4. CIE coordinates of crystals **1**-**3**.

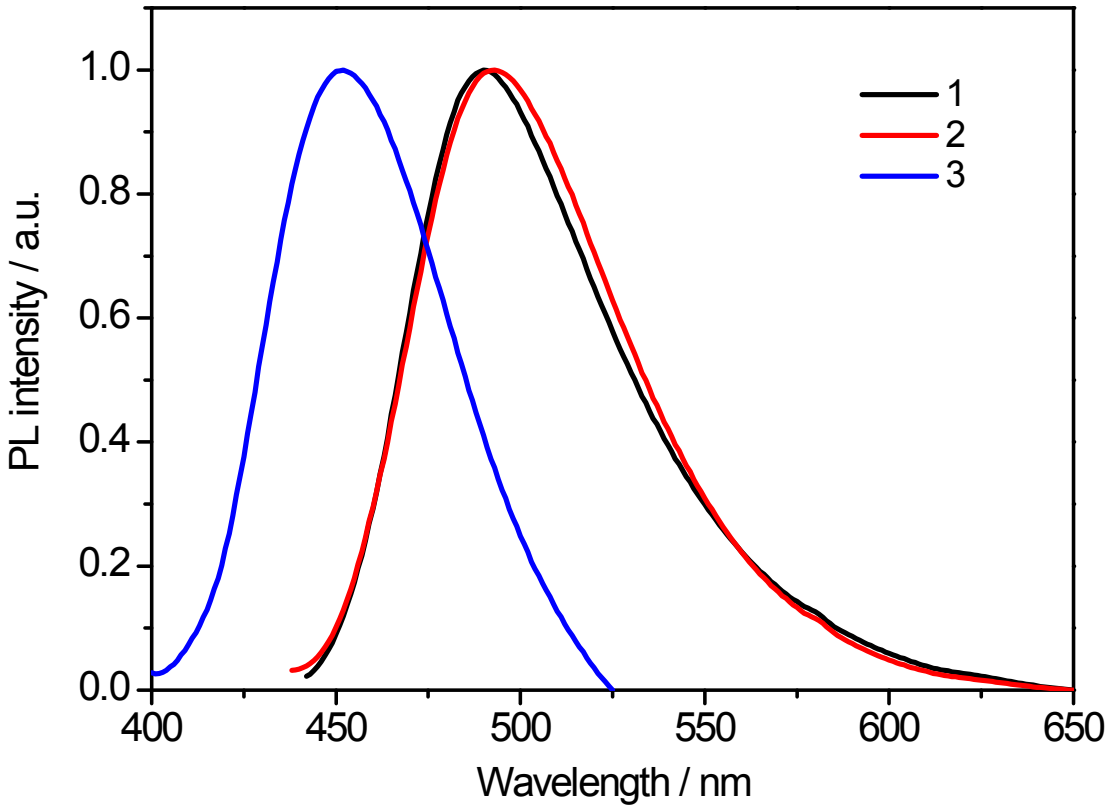

Figure S5. PL spectra of 1-3 doped in PMMA film (10 wt%).

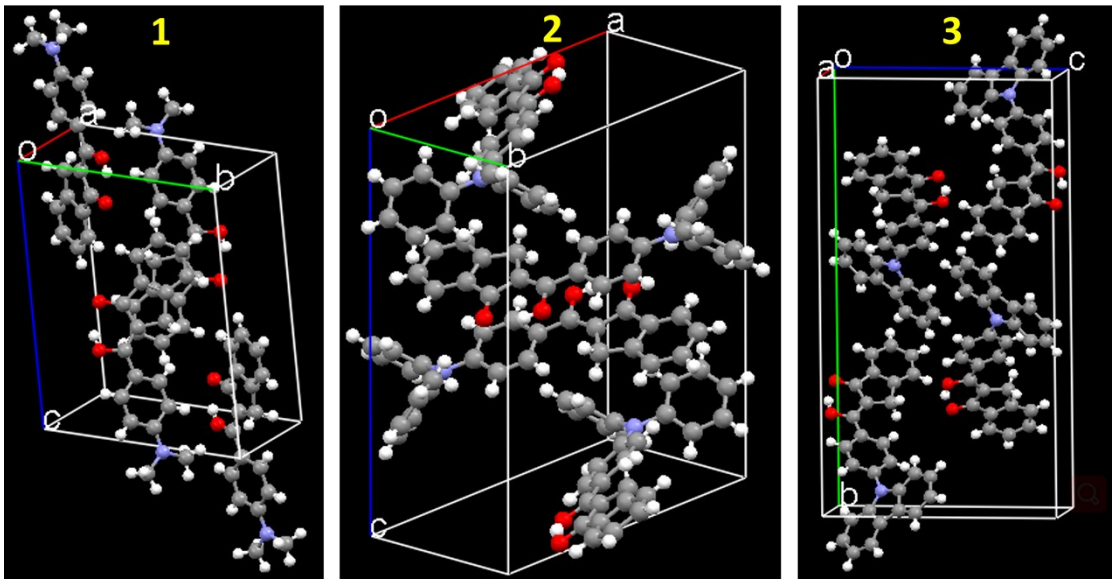

Figure S6. The unit cell of crystals **1**-**3**.

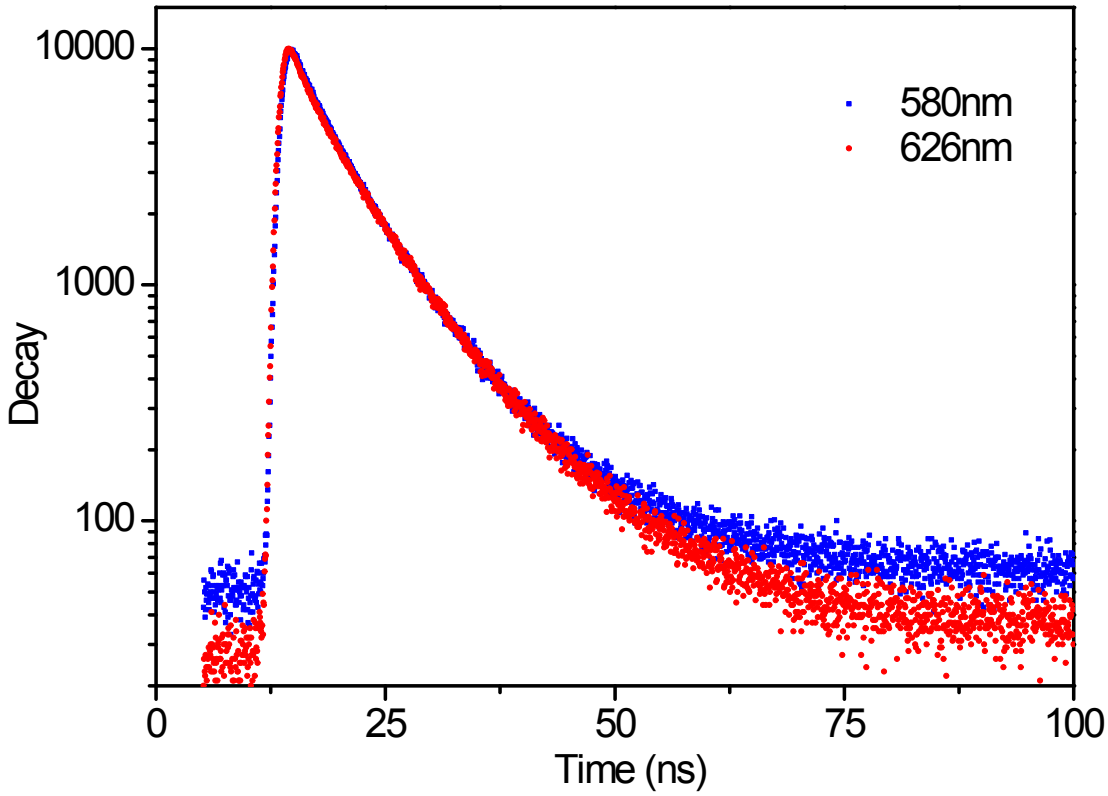

Figure S7. Lifetimes for two different emission bands (580 nm and 626 nm) of compound 1 in crystalline state.

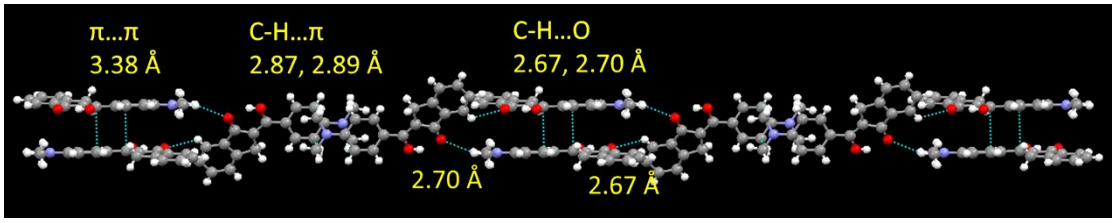

Figure S8. Intermolecular interactions in crystal **1**.

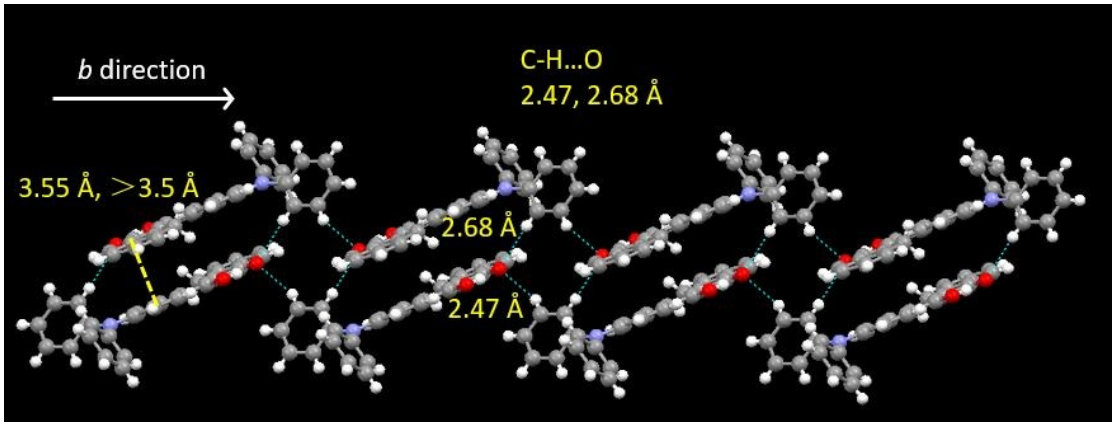

Figure S9. Intermolecular interactions along crystallographic *b* direction in crystal **2**.

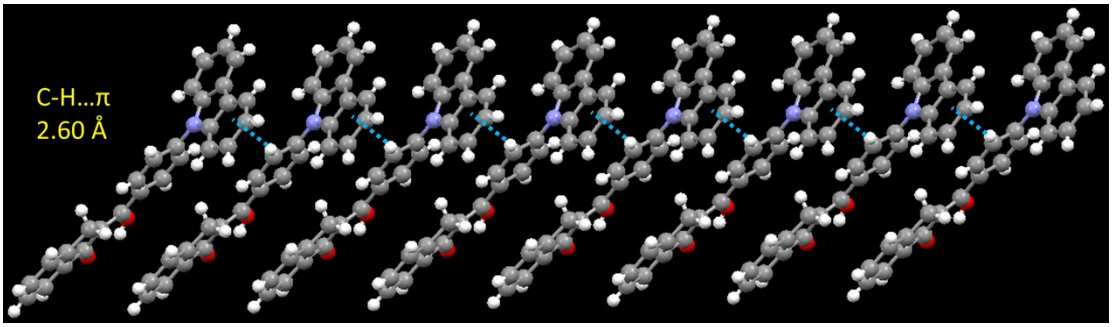

Figure S10. Intermolecular interactions along crystallographic *a* direction in crystal **3**.

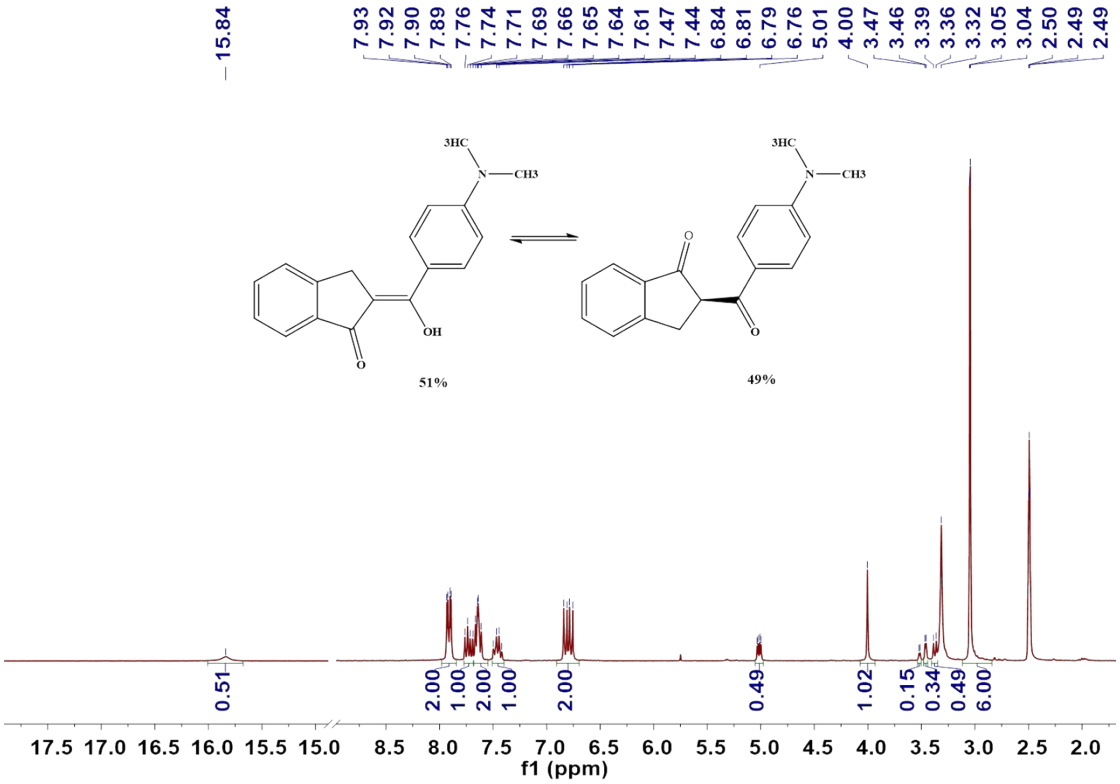

Figure S11. ^{1}H NMR spectrum for compound **1** in DMSO-d6 (500 MHz, 298K).

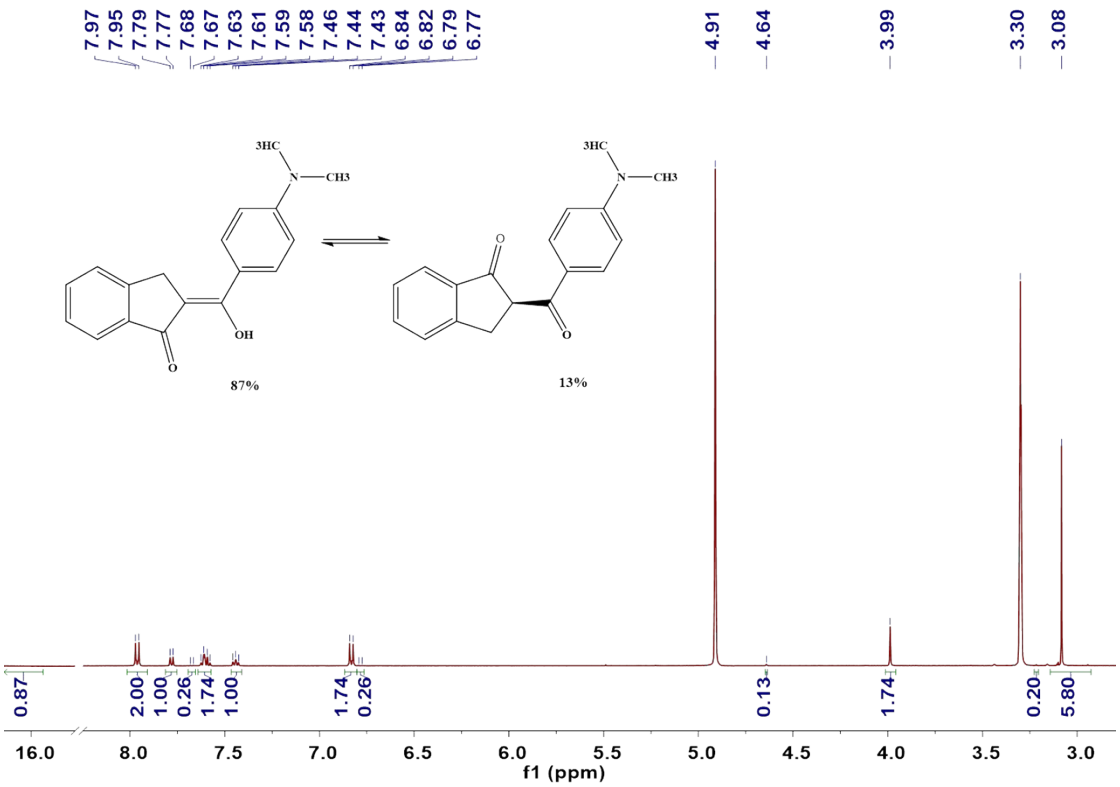

Figure S12. ^{1}H NMR spectrum for compound **1** in Methanol-d4 (500 MHz, 298K).

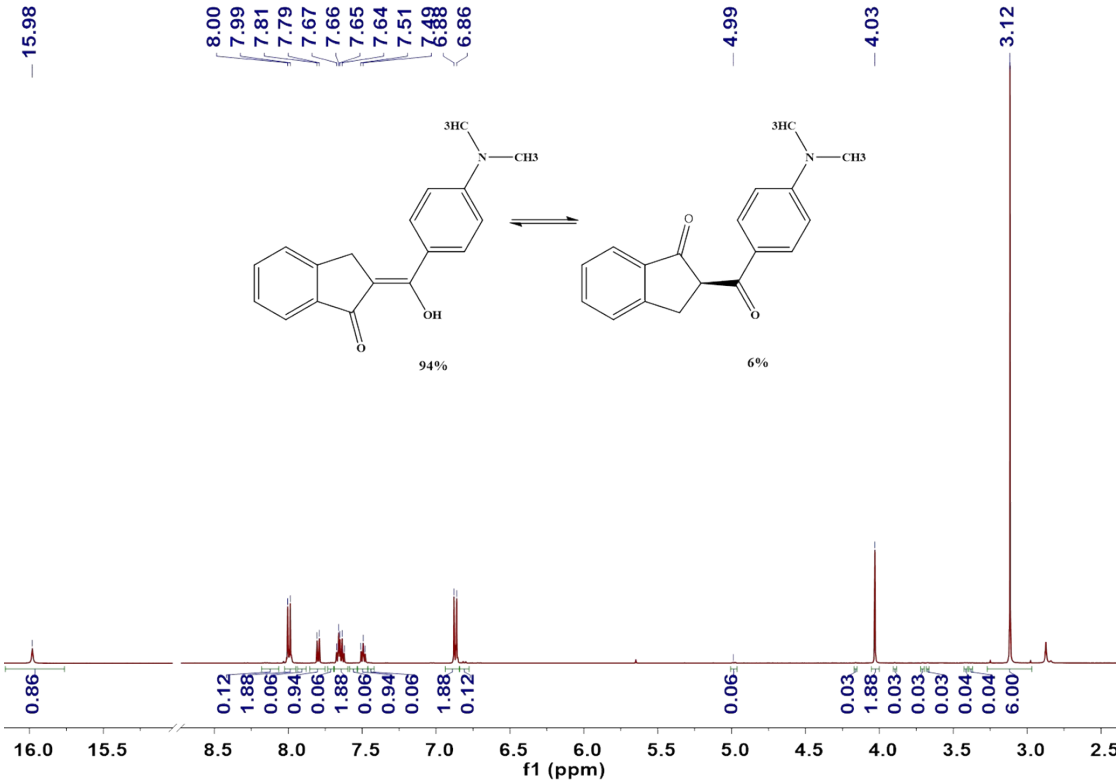

Figure S13. ^{1}H NMR spectrum for compound **1** in Acetone-d6 (500 MHz, 298K).

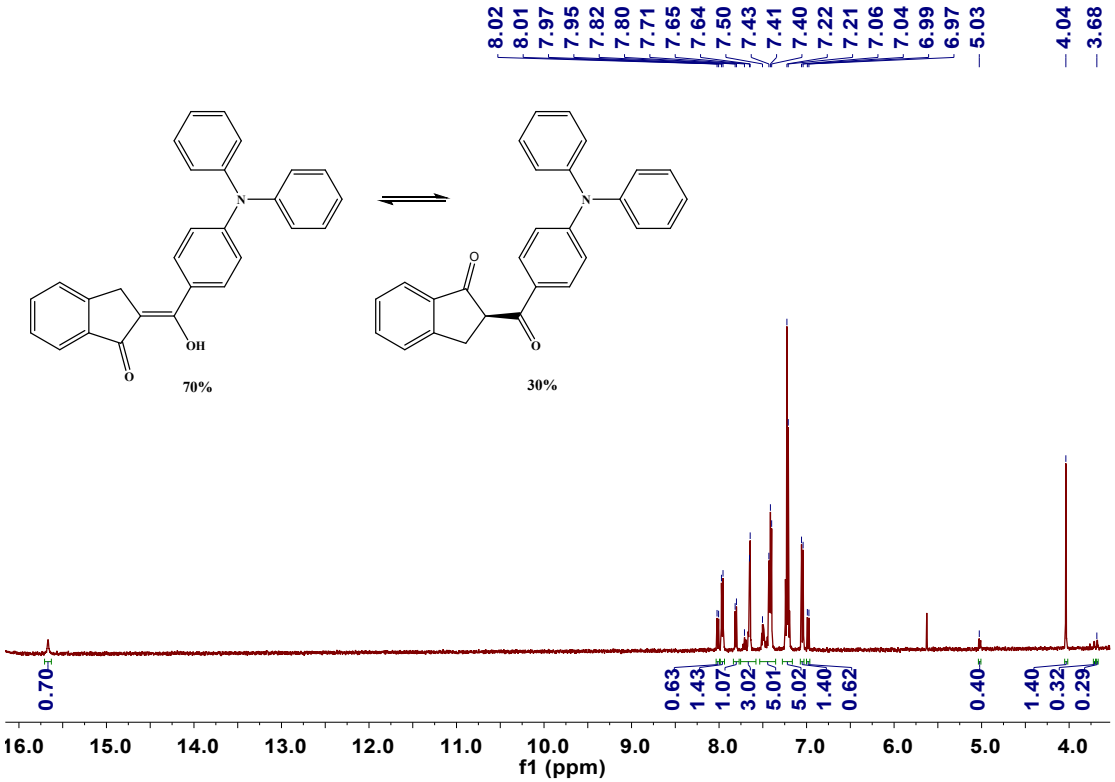

Figure S14. ^{1}H NMR spectrum for compound **2** in Acetone-d6 (500 MHz, 298K).

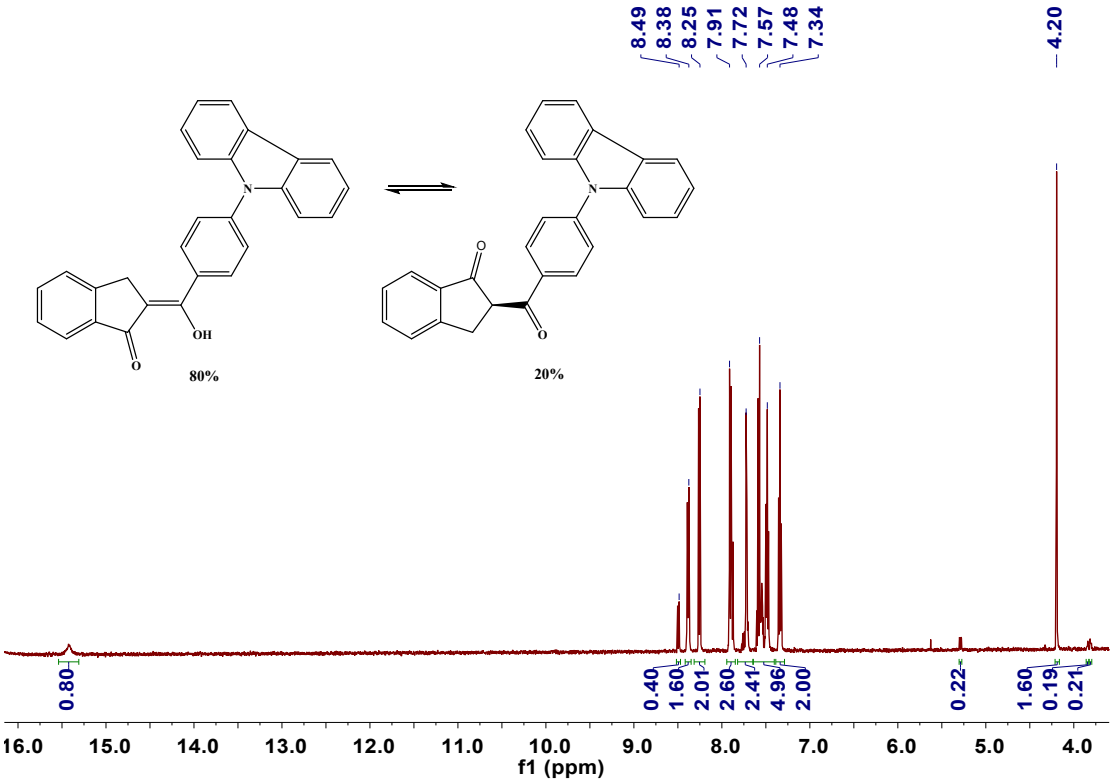

Figure S15. ^{1}H NMR spectrum for compound **3** in Acetone-d6 (500 MHz, 298K).

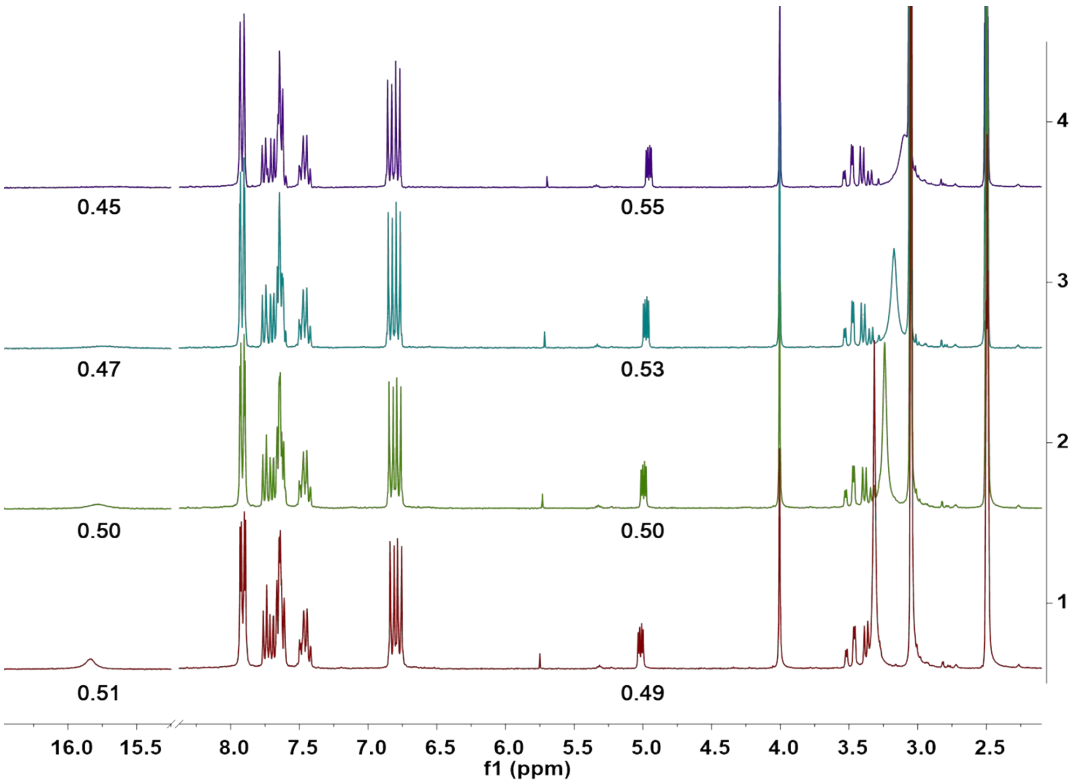

Figure S16. ^{1}H NMR spectrum for compound **1** in DMSO-d6 (300 MHz, 298K for curve 1, 313K for curve 2, 328K for curve 3, 343K for curve 4).

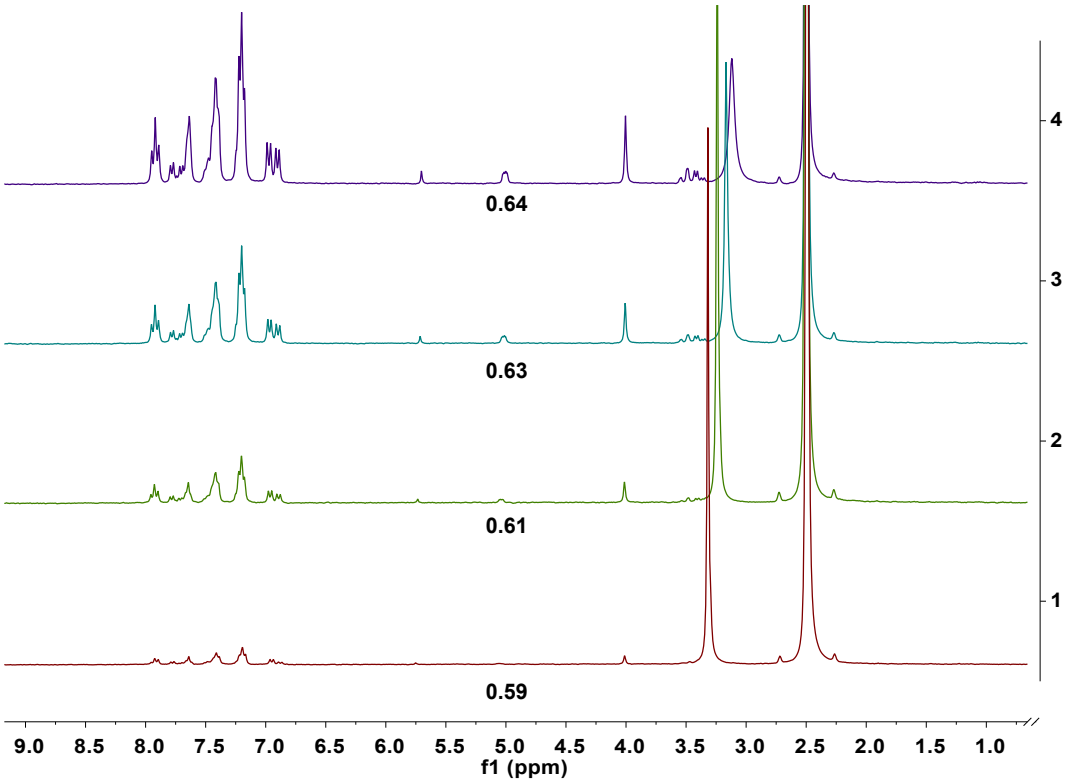

Figure S17. ^{1}H NMR spectrum for compound **2** in DMSO-d6 (300 MHz, 298K for curve 1, 313K for curve 2, 328K for curve 3, 343K for curve 4).

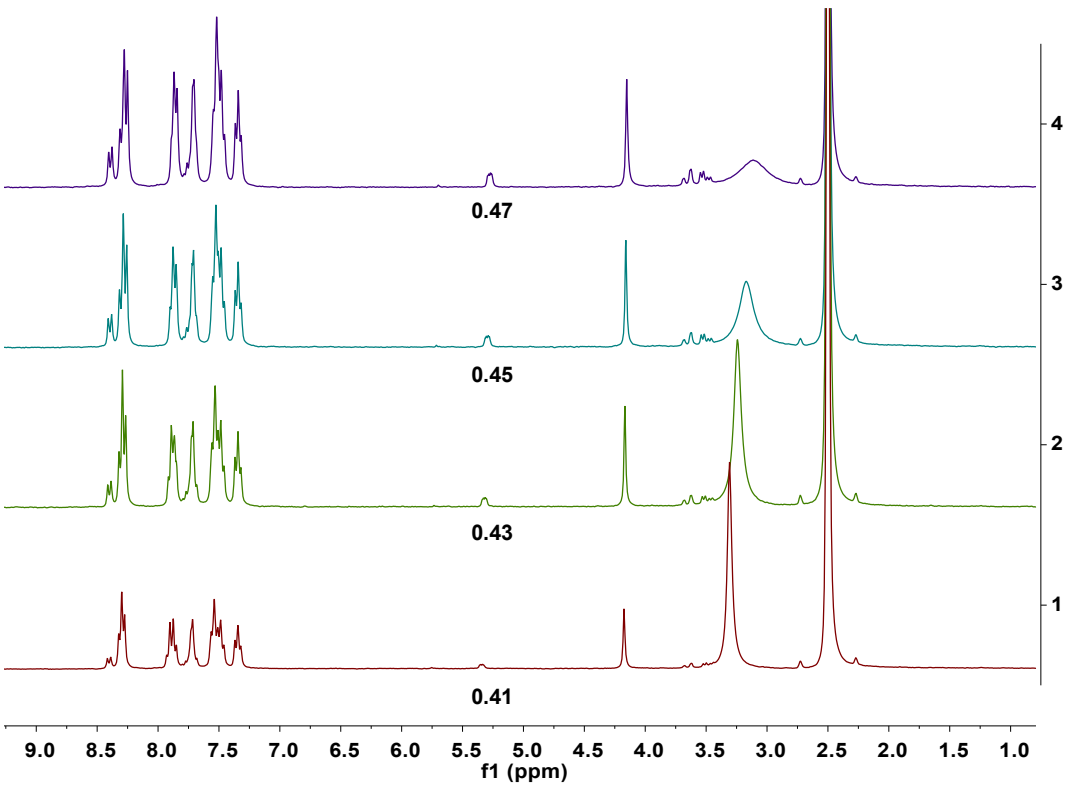

Figure S18. ^{1}H NMR spectrum for compound **3** in DMSO-d6 (300 MHz, 298K for curve 1, 313K for curve 2, 328K for curve 3, 343K for curve 4).

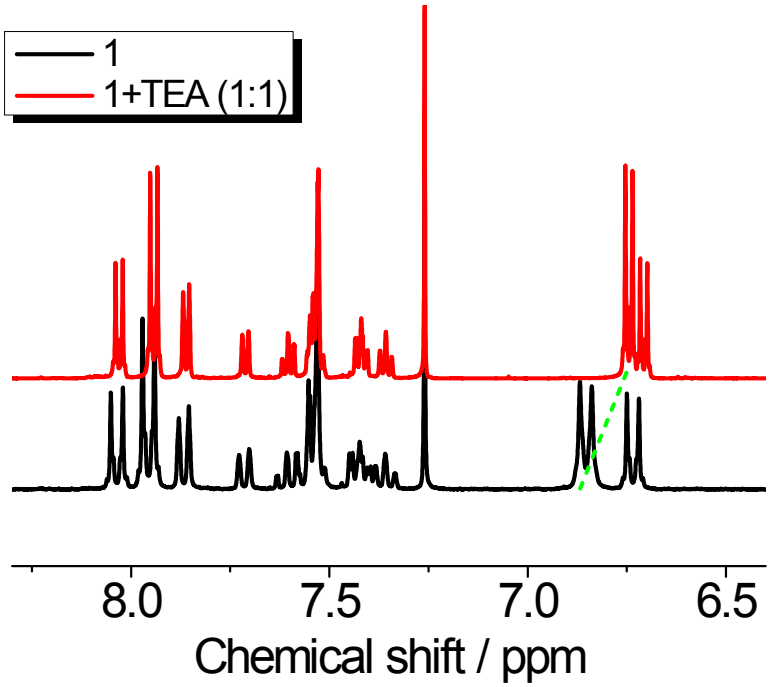

Figure S19. ^{1}H NMR spectrum for compound **1** with Et_3N 1:1 in $CDCl_3$ (500 MHz, 298K).

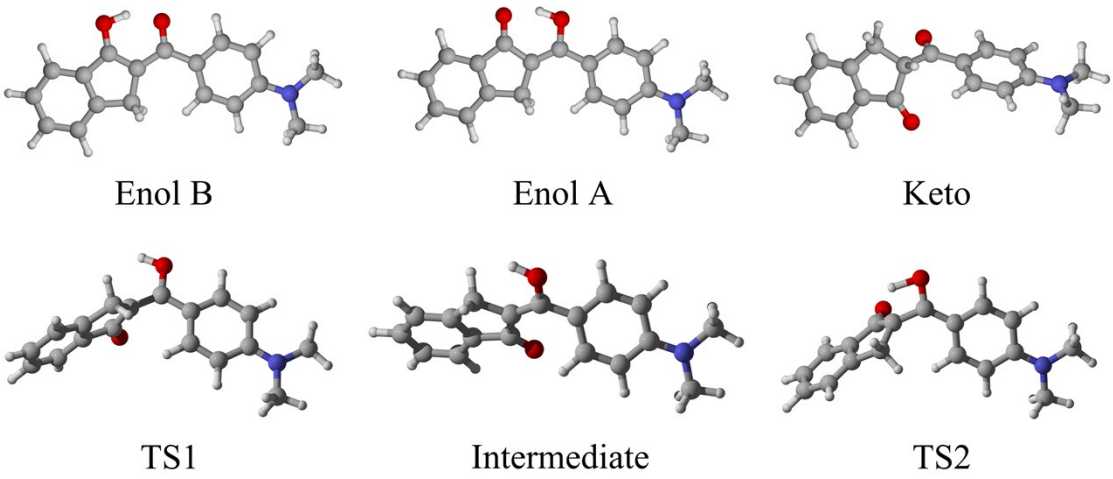

Figure S20. The geometries of 6 forms calculated for compound **1**.

Table S1. The single point energy (a.u.) for Enol A, TS1, Intermediate, TS2 and Keto molecules at different solvents at B3LYP-D3(BJ)/def2-QZVPP level of theory.

Solvents	Enol A	TS1	Intermediate	TS2	Keto
Acetone	-901.8716	-901.7665	-901.8060	-901.7383	-901.8688
Alcohol	-901.8682	-901.8212	-901.8560	-901.7868	-901.8669
Benzene	-901.8675	-901.8035	-901.8493	-901.7798	-901.8629
Chloroform	-901.8204	-901.8119	-901.8534	-901.7841	-901.8162
Dichloromethane	-901.8230	-901.7668	-901.8070	-901.73840	-901.8193
DiethylEther	-901.8694	-901.7593	-901.8022	-901.7339	-901.8655
Formamide	-901.8547	-901.8101	-901.8436	-901.7737	-901.8536
Gas	-901.8447	-901.8222	-901.8558	-901.7865	-901.8390
Methanol	-901.8674	-901.8481	-901.8568	-901.7488	-901.8664
Quinoline	-901.8746	-901.8165	-901.8576	-901.7894	-901.8710
Water	-901.8741	-901.8468	-901.7972	-901.7283	-901.8705
DMSO	-901.8631	-901.8109	-901.8527	-901.7830	-901.8638

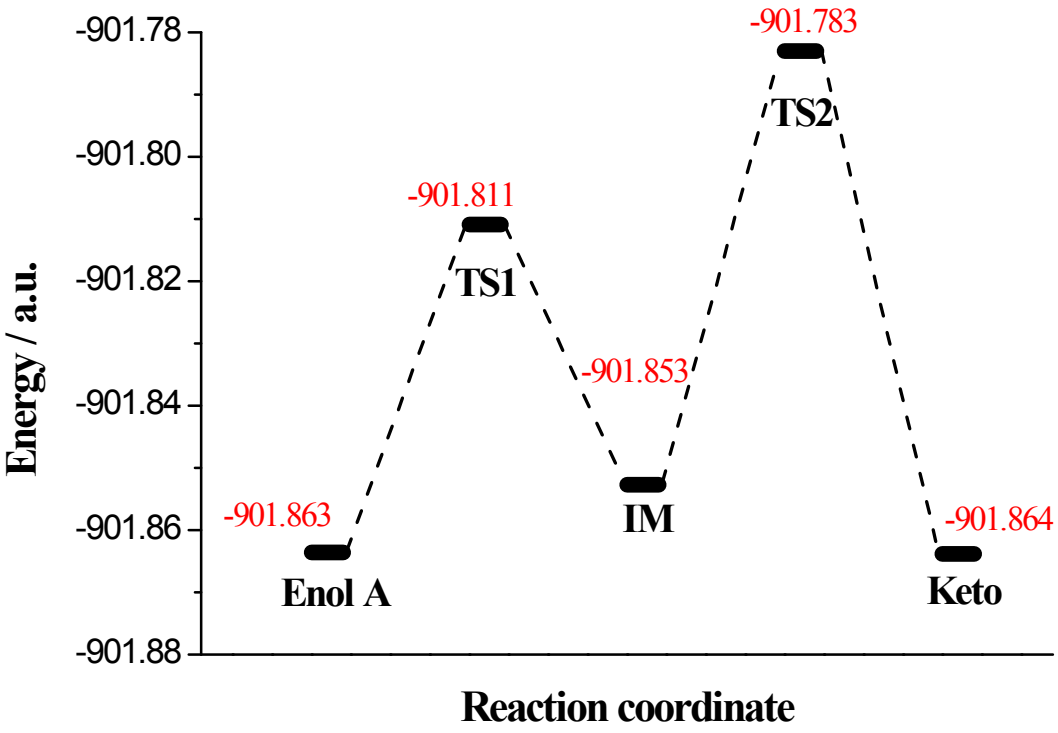

Figure S21. The potential energy surface diagram of compound 1 in DMSO.

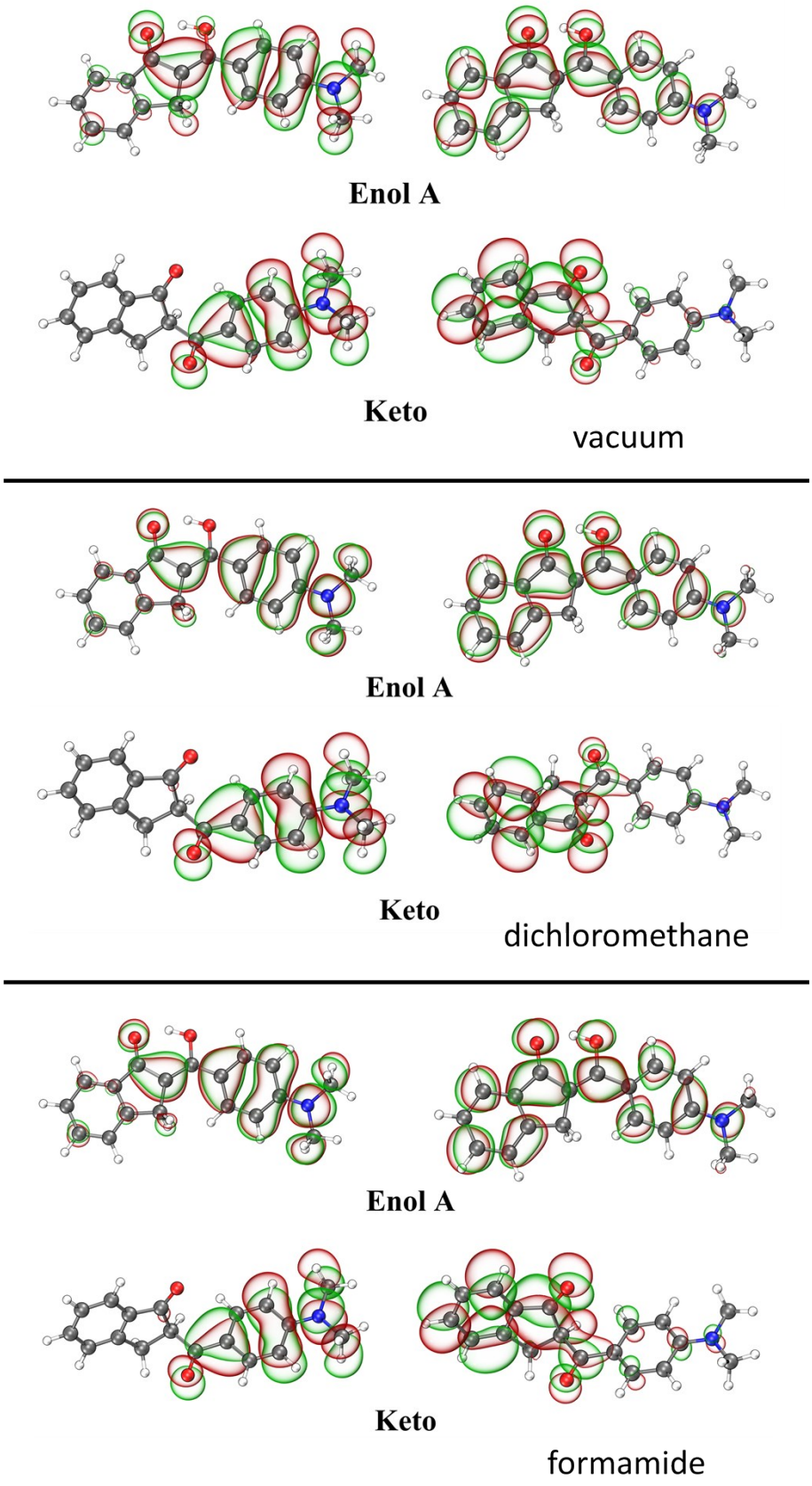

Figure S22. The HOMO (left) and LUMO (right) snapshots for Enol A and Keto forms of compound **1** at vacuum, dichloromethane and formamide. The red and green colors denote positive and negative phases (isovalue=0.02).

Table S2. HOMO, LUMO and their gap (eV) for Enol A and Keto forms at different solvents at B3LYP-D3(BJ)/def2-QZVPP level of theory.

Solvents	Enol A			Keto		
	HOMO	LUMO	gap	HOMO	LUMO	gap
Acetone	-5.3476	-2.0742	3.2734	-5.5131	-1.8235	3.6896
Alcohol	-5.3863	-2.1675	3.2188	-5.5829	-1.9485	3.6343
Benzene	-5.4083	-1.9836	3.4247	-5.5451	-1.7665	3.7786
Chloroform	-5.3780	-2.0418	3.3362	-5.5279	-1.8107	3.7173
Dichloromethane	-5.3599	-2.0627	3.2972	-5.5186	-1.8205	3.6981
DiethylEther	-5.3705	-2.0129	3.3576	-5.5156	-1.7802	3.7354
Formamide	-5.4167	-2.2082	3.2085	-5.5988	-2.0207	3.5781
Gas	-5.5323	-1.9896	3.5427	-5.6729	-1.8073	3.8656
Methanol	-5.3960	-2.1935	3.2025	-5.5981	-1.9800	3.6180
Quinoline	-5.3508	-2.0452	3.3055	-5.5066	-1.7986	3.7080
Water	-5.4106	-2.0963	3.3143	-5.5121	-1.8284	3.6837
DMSO	-5.4237	-2.0187	3.4050	-5.3411	-2.0758	3.2653

Sample Name	ZJX-A	**Position**	P1-F8	**Instrument Name**	Instrument 1	**User Name**	
Inj Vol	-1	**InjPosition**		**SampleType**	Sample	**IRM Calibration Status**	Success
Data Filename	ZJX-A.d	**ACQ Method**	0103.m	**Comment**		**Acquired Time**	10/30/2020 9:24:26 AM

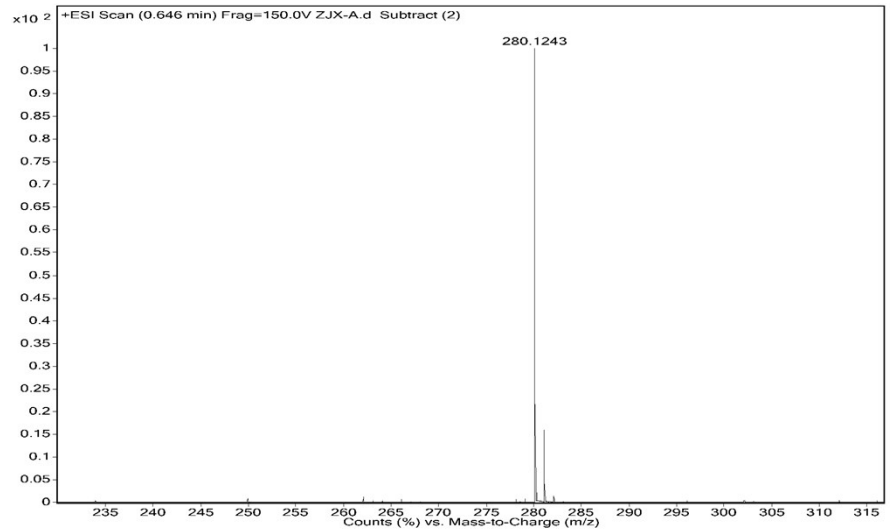

Figure S23. LC/MS spectrum of compound **1**.

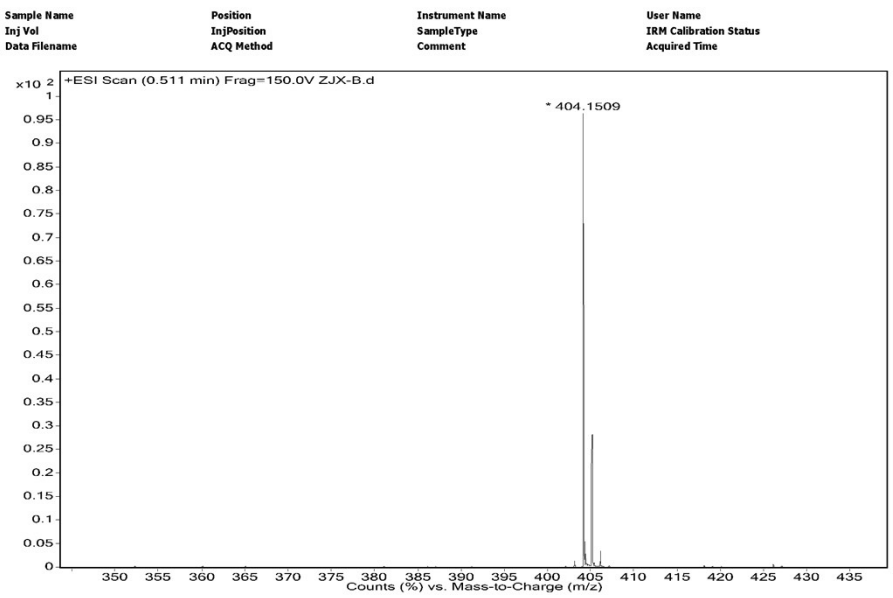

Figure S24. LC/MS spectrum of compound **2**.

Sample Name	ZJX-C1	**Position**	P1-A5	**Instrument Name**	Instrument 1	**User Name**	
Inj Vol	-1	**InjPosition**		**SampleType**	Sample	**IRM Calibration Status**	Success
Data Filename	ZJX-C1.d	**ACQ Method**	0103.m	**Comment**		**Acquired Time**	11/28/2019 8:53:23 AM

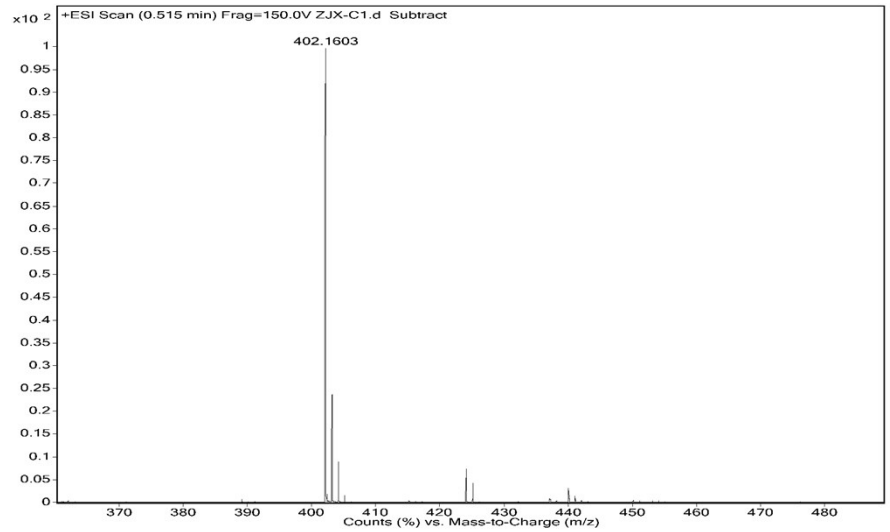

Figure S25. LC/MS spectrum of compound **3**.